Rare Earth Metal Tris(borohydride) Complexes as Initiators for ϵ-Caprolactone Polymerization: General Features and IR Investigations of the Process

Isabelle Palard, Alain Soum, and Sophie M. Guillaume*

Laboratoire de Chimie des Polymères Organiques, (LCPO), CNRS-ENSCPB-Université Bordeaux 1, ENSCPB, 16 Avenue Pey-Berland, 33607 Pessac Cedex, France

Received March 25, 2005; Revised Manuscript Received May 20, 2005

ABSTRACT: Trivalent rare earth metal borohydride complexes $Ln(BH_4)_3(THF)_3$ (Ln = La, Nd, Sm) initiate the ring-opening polymerization of ϵ-caprolactone (ϵ-CL) to give, in quantitative yields and in a few minutes, α,ω-dihydroxytelechelic poly(ϵ-caprolactone) displaying a relatively narrow molar mass distribution (≤1.3). The polymer features depend on both the metal and the solvent. A good agreement between $\bar{M}_{n(theo)}$ and $\bar{M}_{n(exp)}$ is observed for low $[monomer]_0/[initiator]_0$ values whereas a deviation ($\bar{M}_{n(exp)} < \bar{M}_{n(theo)}$) is obtained at higher ratios; this behavior has been rationalized by the occurrence of some transfer reactions. The gel formed during the polymerization arises from the involvement of the $-(OBH_2)$ end groups of the active polymer chains in several inter- and intramolecular van der Waals interactions, as revealed by in-depth infrared investigations of the various intermediates implicated in the whole polymerization mechanism. Finally, the polymers synthesized display only traces of residual nontoxic rare earth metals, thus making them suitable for biomedical applications.

Introduction

As part of our ongoing research in polyesters synthesis initiated by rare earth metal complexes,[1−8] we are paying much attention to developing controlled and living polymerization processes. Our ultimate goal in understanding and mastering the polymerization mechanism is to optimize the process in order to gain access to macromolecular architectures, especially copolymers based on ϵ-caprolactone (ϵ-CL).[5−8]

While the ring-opening polymerization (ROP) of ϵ-CL has been performed with various rare earth metal based initiators, only a few reports claim, based on the successful synthesis of block copolymers, the process to be living.[9−16] Among the undesired side reactions of ROP processes, intramolecular (or backbiting) and intermolecular (or reshuffling) transesterifications are the most common,[3,17−19] but termination and transfer reactions are also encountered.[20] While the former side reactions lead to the formation of cyclic oligomers with a lowering of the polymer molar mass and a broadening of the molar mass distribution ($\bar{M}_w/\bar{M}_n$), the latter ones are usually characterized by either partial monomer conversions or molar mass values lower than those expected. Regarding transfer reactions, these may occur even if the monomer is completely consumed and they lead to experimental molar mass values lower than the theoretical ones as the number of active sites increases.[20]

In our search for an efficient initiator, we have recently reported the versatility of borohydride derivatives $[Ln](BH_4)$ (Ln = rare earth) in ROP of ϵ-caprolactone.[1,2] The trivalent homoleptic $Nd(BH_4)_3(THF)_3$, **Nd-1**, and heteroleptic $(Cp^*)_2Sm(BH_4)(THF)$, **Cp*$_2$Sm-1** ($Cp^* = (\eta\text{-}C_5Me_5)$), complexes successfully allowed the formation of the original α,ω-dihydroxytelechelic poly(ϵ-caprolactone) through a now well-established pseudoanionic coordination−insertion type mechanism. Thanks to the single-site initiator **Cp*$_2$Sm-1**, the intermediates of the process, initially described with the **Nd-1** system, have been better identified and thus confirmed.[1] Noteworthy is that both the steric and electronic contributions of the two "spectator" Cp* ligands appear to slow down the reaction, thereby inducing improved polymerization abilities.[1] Among the side reactions, we have shown that besides minor transesterifications, some other reaction(s) occurred in the polymerization process; with both initiating derivatives **Nd-1** and **Cp*$_2$Sm-1**, while the $\bar{M}_{n(exp)}$ of the poly(ϵ-CL) are in good agreement with the $\bar{M}_{n(theo)}$ at low $[\epsilon\text{-CL}]_0/[BH_4]_0$ ratios,[1,2] a deviation ($\bar{M}_{n(exp)} < \bar{M}_{n(theo)}$) is however observed when this ratio increases.[1] The objective of the present work is first to extend this study of the general features of the polymerization of ϵ-caprolactone initiated by homoleptic borohydride initiators to other rare earth metal derivatives $Ln(BH_4)_3(THF)_3$, Ln = La, **La-1**, Ln = Sm, **Sm-1**. Then, the origin of the observed $\bar{M}_{n(exp)}/\bar{M}_{n(theo)}$ gap is shown to arise from transfer reaction(s).

During the polymerization of ϵ-caprolactone using the borohydride initiators **Ln-1**, as well as **Cp*$_2$Sm-1**, the reaction medium rapidly becomes viscous (within 5 min) to end up as a gel.[1,2] Such a behavior has already been reported during the ROP of cyclic esters by lanthanocene such as $(Cp)_3Ln$ (Ln = Ce, Pr, Sm, Gd, Er)[16] or $Li\{[\eta^{:5}\eta^1C_5R_4(SiMe_2NCH_2CH_2R')_2Ln\}$(Ln = Y, Lu; C_5R = C_5Me_4, C_5H_4, 3-$C_5H_3{}^tBu$; R′ = OMe, NMe_2)[21] or by phosphorane iminato $[La_2(NPPh_3)_4(\mu\text{-}NPPh_3)_2(\mu\text{-}THF)]$ and $[Yb(NPPh_3)_3]_2$ derivatives;[13,22] it has been simply related to the formation of some coordinative polymer network involving coordination of the rare earth metal to the oxygen atoms of the polymer chain. Taking into account the polymerization mechanism,[1,2] we undertook a complete Infrared study of the various intermediates involved in our process, including the active polymer gel, to unveil the nature of the linkage(s) responsible of the cohesion of the gel. Previous reports mentioned the use of IR spectroscopy for the study of the polymerization of ϵ-CL with cationic initiators; however, these only highlighted the complexation of the monomer through the exocyclic oxygen.[23−26] To our knowledge, such com-

* Corresponding author: Phone: (33) (0)5 40 00 84 88; Fax: (33) (0)5 40 00 84 87; E-mail address: guillaume@enscpb.fr.

10.1021/ma0506280 CCC: $30.25
Published on Web 07/02/2005

prehensive IR investigations on the polymerization mechanism of a cyclic ester by a rare earth metal initiator are reported here for the first time. An explanation for the formation of a gel which relies on the participation of the $-(OBH_2)$ active polymer chain end in various van der Waals interactions is thus provided.

Experimental Section

Materials. Due to the sensitivity of the rare earth metal complexes, all manipulations were performed under inert atmosphere (argon, <3 ppm of O_2) by using standard Schlenk, vacuum line, and glovebox techniques. Solvents were thoroughly dried and deoxygenated by standard methods and distilled before use.[27] CD_2Cl_2 was dried over a mixture of 3 and 4 Å molecular sieves. ϵ-Caprolactone (ϵ-CL, Lancaster) was successively dried over CaH_2 (at least 1 week) and 4,4′-methylenebis(phenylisocyanate). IR (neat liquid, cm^{-1}): 2935 vs br, 2863 vs sh, ν(C−H); 2705 vw; 1904 vw, 1832 w; 1724, vs br, ν(C=O); 1291 vs, ν(O−C(O)); 1172 vs, ν(O−CH_2); 1055 vs, 1477 s, 1439 s, 1392 s, 1348 s, 1328 s, 1252 s, 1226 s, 1088 s, 1015 s, 988 s, 963 s, 892 m, 863 s, 849 s, 819 m, 734 m, 696 s. $Ln(BH_4)_3(THF)_3$, Ln = La, Nd, Sm, were synthesized from $LnCl_3$ (Aldrich) following the literature procedure described for $Sm(BH_4)_3(THF)_3$.[28,29] $La(BH_4)_3(THF)_3$, **La-1**: IR (Nujol, cm^{-1}): 3391 w br, 3182 w br, 2724 w, 2676 w; 2434 vs br, 2364 s, 2294 s, 2223 vs br, 2155 vs, ν(B−H); 1686 vw br; 1152 vs br, 1090 vs, δ(B−H); 2969−2954−2853 vs (with Nujol), 1459 vs (with Nujol), 1014 vs, 860 vs br, La-THF; 1345 m, 1296 m, 1250 m, 1036 s, 961 s, 919 s, 669 s. $Nd(BH_4)_3(THF)_3$, **Nd-1**: IR (Nujol, cm^{-1}): 3392, w br, 3314 w br, 3187 w; 2723 w, 2695 w; 2438 vs br, 2329 vs br, 2225 vs br, 2160 vs br, 1873 w, ν(B−H); 1692 w br; 1153 vs br, 1091 vs br, δ(B−H); 1344 vs; 3000−2828 vs (with Nujol), 1456 s (with Nujol), 1013 vs, 862 vs br, Nd-THF; 1344 s, 1296 s, 1250 s, 1032 s, 960 s, 919 s, 668 s. $Sm(BH_4)_3(THF)_3$, **Sm-1**: IR (Nujol, cm^{-1}): 3331 w br, 3188 vw br, 2723 vw, 2694 vw; 2454 vs br, 2391 vs br, 2299 vs br, 2217 vs br, 2150 vs br, ν(B−H); 1687 vw br; 1167 vs br, 1091 vs br, δ(B−H); 3000−2844 vs (with Nujol), 1459 (with Nujol) vs, 1008 vs, 854 vs br, Sm-THF; 1344 s, 1298 s, 1248 s, 1039 s, 955 m, 919 s, 671 s. All other reagents were commercially available (Aldrich).

Instrumentation and Measurements. ^1H (400 MHz) and ^{13}C (100 MHz) NMR spectra were recorded in CD_2Cl_2 on a Bruker Avance DPX 400 at 23 °C and were referenced internally using the residual ^1H and ^{13}C solvent resonance relative to tetramethylsilane ($\delta = 0$).

Average molar mass ($\bar{M}_n$) and molar mass distribution ($\bar{M}_w/\bar{M}_n$) determinations were performed in THF at 20 °C (flow rate 0.8 mL·min^{-1}) on a Varian apparatus equipped with a refractive index detector and four TSK gel columns with successively 250, 1500, 10^4, and 10^5 Å pore sizes and 5 μm bead size. The polymer samples were dissolved in THF (2 mg·mL^{-1}). $\bar{M}_n$ values were calculated from the linear polystyrene calibration curve using the correction coefficient previously reported ($\bar{M}_{n(exp)} = 0.56\bar{M}_{n(SEC)}$).[4] This coefficient has been confirmed upon comparing the calculated molar mass ($\bar{M}_{n(exp)}$) to the real ones measured either by ^1H NMR ($\bar{M}_n$< 10 000) or by osmometry ($\bar{M}_n$ > 10 000) and by SEC equipped with a refractive index detector coupled to a viscosimeter (Gonotec-Osmomat 090). Molar masses < 10 000 were also calculated from ^1H NMR analyses; the values resulted from the integration ratio of the main chain signal (OCH_2, 2nH) at $\delta = 4.05$ ppm relative to the end group methylene proton signal (CH_2OH, 4H) at $\delta = 3.64$ ppm. The molar mass distributions have been calculated from SEC chromatogram traces. The monomer conversion was calculated from ^1H NMR spectra of the crude polymer sample from the integration (Int.) ratio Int.P(ϵ-CL)/[Int.P(ϵ-CL) + Int.(ϵ-CL)] using the methyl group in α of the carbonyl ($CH_2C(O)$). The polymer yield was obtained by gravimetric measurements of the precipitated polyester.

Infrared spectra ranging from 600 to 4000 cm^{-1} were recorded under argon either neat or in mineral oil using KBr plates or as KBr pellets on a Bruker Tensor spectrometer with a 4 cm^{-1} resolution. For clarity, the Nujol absorption bands (neat, cm^{-1}: 2924 vs, 2854 vs; 1461 s, 1377 m, 722 w) have been omitted; only those overlapping with the product are mentioned.

Elemental analyses have been performed by the Analytische Laboratorien at Lindlar, Germany.

Typical Polymerization Procedure. Under vacuum, a 1.5 M solution of ϵ-CL (0.5 mL, 4.5 mmol) in toluene (2.5 mL) was added via a buret to a CH_2Cl_2 (1 mL) stirred solution of **Ln-1** (4−6 mg, 8−11 μmol) at 21 °C. A gel (colorless with **La-1** and **Sm-1**, bluish with **Nd-1**) was systematically formed within 10 min. The polymerization was then stopped after 5/15 min by addition of a large excess, relative to **Ln-1**, of an acetic acid solution (16.5×10^{-3} mol L^{-1} in toluene); finally, the resulting mixture was dried and the conversion determined by NMR analysis. This crude polymer was dissolved in CH_2Cl_2, purified upon precipitation in a large amount of cold pentane followed by centrifugation and finally dried under dynamic vacuum. The resulting polymers were then characterized by ^1H and ^{13}C NMR, SEC and MALDI−TOF MS analyses.

Synthesis of $Ln[O(CH_2)_6(OBH_2)]_3$, Ln-2. All **Ln-2** samples were prepared upon reacting **Ln-1** (Ln = La: 218 mg; 0.545 mmol) with 3 equiv of ϵ-CL (slight default, 180 μL; 1.624 mmol) in THF (5 mL) at 21 °C. A white precipitate rapidly (∼5 min) falls out in a colorless solution. After the mixture was stirred for over 1 h, the precipitate was washed with THF and dried to afford **Ln-2** (Ln = La: 94% yield, 260 mg, 494 μmol). This insoluble solid has been characterized by elemental and IR analyses. $La[O(CH_2)_6(OBH_2)]_3$, **La-2**: Anal. Calcd for $C_{18}H_{42}B_3LaO_6$: C 41.11; H 8.05; B 6.17; Found: C 40.87; H 8.00; B 6.20. IR (Nujol, cm^{-1}): 3375 w br, 3172 w br, ν(O−H); 2725 m, 2681 m, ν(C−H); 2423 m, 2373 m, 2293 m, 2225 m, 2160 m, ν(B−H); 1734 w, ν(C=O); 1665 w; 1261 s, 1228 s; 1155 s, 1056 vs br, δ(B−H); 744 m, 681 m, 667 m. $Nd[O(CH_2)_6(OBH_2)]_3$, **Nd-2**: synthesized as previously described.[2] IR (Nujol, cm^{-1}): 3331 w br, 3166 w br, ν(O−H); 2725 m, 2679 m br, ν(C−H); 2427 m br, 2357 m, 2331 m, 2290 m, 2212 m, 2160 m, 2048 w br, ν(B−H); 1736 vw, ν(C=O); 1654 m br; 1262 vs, 1220 s; 1120 s, 1069 vs br, δ(B−H); 808 w, 770 w, 691 w, 666 m. $Sm[O(CH_2)_6(OBH_2)]_3$, **Sm-2**: Anal. Calcd for $C_{18}H_{42}B_3SmO_6$: C 40.24; H 7.88; B 6.04; Found: C 40.51; H 7.70; B 5.84. IR (Nujol, cm^{-1}): 3352 w br, 3180 w br, ν(O−H); 2726 m, 2672 m br, ν(C−H); 2439 m br, 2344 m, 2294 m, 2222 m, 2163 m, ν(B−H); 1734 vw, ν(C=O); 1655 vw; 1262 vs, 1223 s; 1167 s, 1058 vs br, δ(B−H); 769 m, 666 s.

Synthesis of $Ln[\{O(CH_2)_5C(O)\}_nO(CH_2)_6(OBH_2)]_3$, Ln-3. In the glovebox, a THF solution (2 mL) of ϵ-CL (0.2 mL; 1.80 mmol) is added to a THF solution (0.9 mL) of **Ln-1** (Ln = La: 5 mg; 12.5 μmol). When the mixture was stirred for over 5 min, a clear gel formed. It was then analyzed by IR spectroscopy. $La[\{O(CH_2)_5C(O)\}_{46}O(CH_2)_6(OBH_2)]_3$, **La-3**. IR ($[\epsilon\text{-CL}]_0/[BH_4]_0 = n + 1 = 47$) (neat, cm^{-1}): 3927 m, 3786 m vbr; 3567 w, 3454 w, ν(O−H); 2721 s, 2683 s, 2654 s, ν(C−H); 2601 m, 2550 m; 2361 m, 2290 m, 2278 m, 2202 m, 2133 m, 2097 m, ν(B−H); 1967 s sh; 1735 vs sh, ν(C=O); 3016−2807 vs (with Nujol), 1456 vs (with Nujol), 1069 vs br, 911 vs br, free THF; 1395 s, 1363 s; 1335 s br, 1242 s br, 1164 vs vbr, δ(B−H); 736 m, 658 vs. $Nd[\{O(CH_2)_5C(O)\}_{60}O(CH_2)_6(OBH_2)]_3$, **Nd-3**. IR ($[\epsilon\text{-CL}]_0/[BH_4]_0 = n + 1 = 61$) (neat, cm^{-1}): 3926 w, 3785 w; 3449 w vbr, 3241, w br, ν(O−H); 2721 m, 2682 s, 2654 m, ν(C−H); 2601 m, 2550 w; 2364 w, 2292 w, 2202 w, 2127 w, 2096 w, ν(B−H); 1967 m; 1737 vs sh, ν(C=O); 3000−2828 vs (with Nujol), 1460 vs br (with Nujol), 1078 vs br, 910 vs br, free THF; 1406 s, 1364 s, 1333 s; 1289 s, 1238 s, 1173 vs, br, δ(B−H); 736 m, 658 s. $Sm[\{O(CH_2)_5C(O)\}_{80}O(CH_2)_6(OBH_2)]_3$, **Sm-3**. IR ($[\epsilon\text{-CL}]_0/[BH_4]_0 = n + 1 = 81$) (neat, cm^{-1}): 3926 w, 3785 w; 3562 w, 3453 w, ν(O−H); 2721 s, 2682 s, 2654 s, ν(C−H); 2601 m, 2550 w; 2363 w, 2293 w, 2202 w, 2132 w, 2096 w, ν(B−H); 1967 s; 1737 vs, ν(C=O); 2995−2813 vs (with Nujol), 1461 vs (with Nujol), 1056 vs br, 902 vs br, free THF; 1397 s, 1391 vs, 1364 s; 1293 s, 1238 s, 1170 vs vbr, δ(B−H); 736 m, 658 s. Assignments of the ν(B−H) and δ(B−H) bands in **Ln-3** have been derived from the analysis of **Ln-1** and **Ln-2** complexes.

$\mathbf{HO(CH_2)_5C(O)\{O(CH_2)_5C(O)\}_{39}O(CH_2)_6OH}$ ($[\epsilon\text{-CL}]_0/[BH_4]_0 = n + 2 = 41$) was synthesized as previously described.[1,2] IR

Scheme 1. Compound Formulas and Numbering

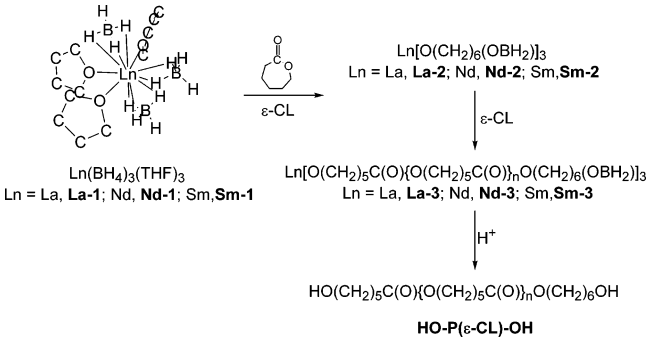

Table 1. Polymerization of ϵ-CL in THF Initiated by La(BH$_4$)$_3$(THF)$_3$, La-1 ([ϵ-CL]$_0$ = 1128 mmol L^{-1}; Monomer Conversion = 100%)

[ϵ-CL]$_0$/[BH$_4$]$_0$[a]	[**La-1**]$_0$ (mmol L^{-1})	reacn time (min)	$\bar{M}_{n(theo)}$[b] (g mol^{-1})	$\bar{M}_{n(exp)}$ (g mol^{-1})	$\bar{M}_w/\bar{M}_n$
251	1.5	15	28614	24450	1.2
130	2.9	15	14820	12800	1.2
77	4.9	5	8778	6800	1.2
54	7.0	5	6156	5100	1.1
35	10.6	5	3990	4200	1.1

[a] [BH$_4$]$_0$ = 3[**La-1**]$_0$ = 3[La(BH$_4$)$_3$(THF)$_3$]$_0$. [b] Calculated for three growing polymer chains per lanthanum atom with $\bar{M}_{n(theo)}$ = [ϵ-CL]$_0$/[BH$_4$]$_0$ × 114.

Table 2. Polymerization of ϵ-CL in THF Initiated by Nd(BH$_4$)$_3$(THF)$_3$, Nd-1 (Monomer Conversion = 100%)

[ϵ-CL]$_0$/[BH$_4$]$_0$[a]	[Nd-1]$_0$ (mmol L^{-1})	[ϵ-CL]$_0$ (mmol L^{-1})	reacn time (min)	$\bar{M}_{n(theo)}$[b] (g mol^{-1})	$\bar{M}_{n(exp)}$ (g mol^{-1})	$\bar{M}_w/\bar{M}_n$
221	1.7	1128	15	25194	17000	1.4
179	2.1	1128	15	20406	15000	1.3
116[2]	6.0	2090	5	13224	10300	1.2
85[2]	4.6	1170	5	9690	8300	1.4
78	4.8	1128	5	8892	7000	1.2
60[2]	9.2	1650	5	6840	5450	1.3
51[2]	7.7	1170	5	5814	4900	1.3
33[2]	12.5	1250	5	3762	3500	1.2

[a] [BH$_4$]$_0$ = 3[**Nd-1**]$_0$ = 3[Nd(BH$_4$)$_3$(THF)$_3$]$_0$. [b] Calculated for three growing polymer chains per neodymium atom with $\bar{M}_{n(theo)}$ = [ϵ-CL]$_0$/[BH$_4$]$_0$ × 114.

(KBr pellet, cm^{-1}): 3538 m br; 3440 m, ν(O−H); 2948 vs br, 2868 vs sh ν(C−H); 2346 w, 2093 w; 1728, vs br, ν(C=O); 1175 vs br, ν(O−CH$_2$); 1295 vs, 1241 vs, ν(O−C(O)); 1473 s, 1420 s, 1398 s, 1366 s, 1108 s, 1047 s, 961 s, 934 m, 840 m, 773 w, 732 s, 710 m.

Results and Discussion

A. Characteristics of the Polymerization of ϵ-Caprolactone Initiated by Ln(BH$_4$)$_3$(THF)$_3$. General Data. The trifunctional rare earth metal borohydride complexes Ln(BH$_4$)$_3$(THF)$_3$ (Ln = La, **La-1**; Ln = Nd, **Nd-1**; Ln = Sm, **Sm-1**) (Scheme 1) initiate the ring-opening polymerization of ϵ-caprolactone, in THF, at room temperature (21 °C), with a remarkable efficiency (Tables 1−3). The monomer conversion is quantitative within 5−15 min depending on [BH$_4$]$_0$. Moreover, as previously reported with (Cp*)$_2$Sm(BH$_4$)(THF), **Cp*$_2$Sm-1**, the occurrence of inter- or intramolecular transesterification reactions remains negligible since besides the crude polymer, less than 5% oligomers are obtained and no variation with time of the molar mass and molar mass distribution is observed.

At low [ϵ-CL]$_0$/[BH$_4$]$_0$ ratios, $\bar{M}_{n(exp)}$ values (calculated from both SEC and NMR analyses) are in agreement with the theoretical ones $\bar{M}_{n(theo)}$ (calculated from the initial concentration in rare earth metal complex on the basis of three active sites[30,31] per metal available for polymerization with [BH$_4$]$_0$ = 3[**Ln-1**]$_0$).[58] However, at higher ratios, a deviation is observed ($\bar{M}_{n(exp)} < \bar{M}_{n(theo)}$; Figures 1−3) while the molar mass distribution remains rather narrow ($1.1 < \bar{M}_w/\bar{M}_n < 1.5$) over the whole range of initiator concentration. A comparable difference between $\bar{M}_{n(exp)}$ and $\bar{M}_{n(theo)}$ has also been mentioned by Greiner for the polymerization of ϵ-CL initiated by the samarium phosphorane iminato species, Sm$_2$I(NPPh$_3$)$_5$(DME).[15,22] In this case, a plateau was reached at [ϵ-CL]$_0$/[initiator]$_0$ > 350 but no explicit explanation was given. Since the contribution of transesterification reactions can be considered as negligible and since $\bar{M}_{n(exp)} < \bar{M}_{n(theo)}$, the discrepancy should arise from the presence of more than the three expected growing chains per rare earth metal center on the trifunctional initiator (Table 4). Therefore, the deviation observed might be due to the occurrence of transfer reaction(s). These would result from the formation of (a) new active

Table 3. Polymerization of ϵ-CL in THF Initiated by Sm(BH$_4$)$_3$(THF)$_3$, Sm-1 ([ϵ-CL]$_0$ = 1128 mmol L^{-1}; Monomer Conversion = 100%)

[ϵ-CL]$_0$/[BH$_4$]$_0$[a]	[Sm-1]$_0$ (mmol L^{-1})	reacn time (min)	$\bar{M}_{n(theo)}$[b] (g mol^{-1})	$\bar{M}_{n(exp)}$ (g mol^{-1})	$\bar{M}_w/\bar{M}_n$
235	1.6	15	26790	21400	1.3
179	2.1	15	20406	16600	1.3
87	4.3	5	9918	7250	1.2
54	6.9	5	6156	4900	1.3
42	9.0	5	4788	3450	1.1

[a] [BH$_4$]$_0$ = 3[**Sm-1**]$_0$ = 3[Sm(BH$_4$)$_3$(THF)$_3$]$_0$. [b] Calculated for three growing polymer chains per samarium atom with $\bar{M}_{n(theo)}$ = [ϵ-CL]$_0$/[BH$_4$]$_0$ × 114.

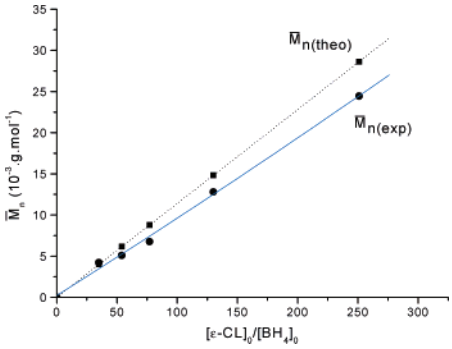

Figure 1. Variations of the theoretical and experimental molar mass values vs [ϵ-CL]$_0$/[BH$_4$]$_0$ for the polymerization of ϵ-CL initiated by La(BH$_4$)$_3$(THF)$_3$, **La-1** (refer to Table 1 for experimental conditions).

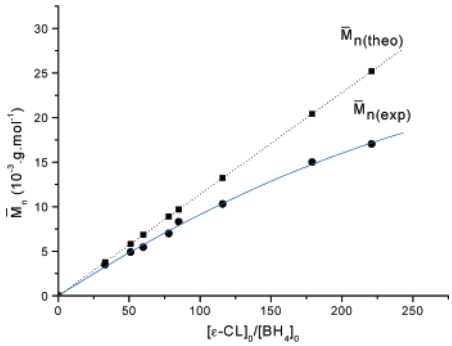

Figure 2. Variations of the theoretical and experimental molar mass values versus [ϵ-CL]$_0$/[BH$_4$]$_0$ for the polymerization of ϵ-CL initiated by Nd(BH$_4$)$_3$(THF)$_3$, **Nd-1** (refer to Table 2 for experimental conditions).

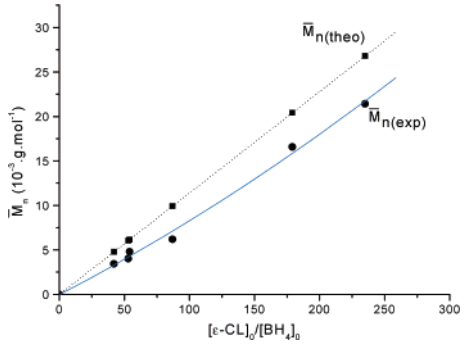

Figure 3. Variations of the theoretical and experimental molar mass values vs $[\epsilon\text{-CL}]_0/[BH_4]_0$ for the polymerization of ϵ-CL initiated by $Sm(BH_4)_3(THF)_3$, **Sm-1** (refer to Table 3 for experimental conditions).

species, such as a putative rare earth metal hydride or alkoxide, through a side reaction involving the $-(OBH_2)$ chain end of the active polymer chain $Ln[\{O(CH_2)_5C(O)\}_nO(CH_2)_6O(BH_2)]_3$ (vide infra). Indeed, both hydride and alkoxide rare earth metal complexes are known to polymerize lactones.[9−12]

Metal Effect. The nature of the rare earth metal in $Ln(BH_4)_3(THF)_3$, **Ln-1**, initiators has an effect on the polymerization of ϵ-CL. Experimentally, lanthanum gives the best results in terms of control (La > Sm > Nd). Indeed, with **La-1**, the polymer experimental molar mass values display the best agreement with the calculated ones (the overall deviation is slightly weaker with **La-1** compared to **Sm-1** and **Nd-1**, La < Sm < Nd) while the molar mass distributions exhibit the smallest values (compared to those obtained with **Sm-1** and **Nd-1**) (Tables 1−3).

Some authors have evaluated the size effect of the metal of a given rare earth metal initiator on the efficiency for controlling the polymerization of cyclic esters.[14,16,23,32−39] On one hand, the order of reactivity follows the size of the metal with the larger lanthanum being more efficient and lutetium, the smallest metal, giving the poorest results. However, when one considers the corresponding molecular mass distributions, these are worse for larger metals and closest to unity with the smallest ones[23,32,35−37] such that a medium-size rare earth metal would afford the best compromise between control and narrow molar mass distribution.[16,23,32−39,59] On the other hand, similarly to our results, Agarwal (among others) has reported that the order of control efficiency of $(Cp)_3Ln$ initiators ($Cp = \eta$-C_5H_5) is opposite (Er ∼ Gd > Sm > Pr > Ce) to the order of the ionic radius of the metals.[11,16,34]

The comparison of the metal influence thus seems to be feasible only within a series of analogous initiators. These observations suggest that an initiator performances in polymerization is governed not only by the nature of the rare earth metal but also by the ancillary ligands present in the coordination sphere of the metal which do play a significant role, as already pointed out.[1,11,39−41]

Solvent Effect. To evaluate the effect of the reaction medium on the process, we performed the polymerization of ϵ-CL using $Sm(BH_4)_3(THF)_3$, **Sm-1**, in CH_2Cl_2/toluene or CH_3CN (Tables 5 and 6) and compared the results to those obtained in THF (Table 3). The polymers formed in THF exhibited slightly narrower molar mass distributions (1.1−1.3) compared to those observed in noncoordinating solvents CH_2Cl_2/toluene (1.3−1.5). In a coordination−insertion type polymerization mechanism, the monomer has to compete with the coordinating solvent for complexation to the metallic center. Even though THF has a weaker coordinating power than ϵ-CL,[42] it is in excess (10-fold) relative to the monomer and the competition is indeed real. Therefore, using a coordinating solvent such as THF would then have the propensity to slow the reaction, to improve the control and to lower molar mass distributions.[15,16,40,41,43] Earlier work on $\{Sm[N(SiMe_3)_2]_2(\mu\text{-Br})\}_2$ revealed that addition (10−20%) of THF or DME to toluene improves the initiator solubility and reduces the polymerization rate as a result of the THF-DME/ϵ-CL competition for coordination to the metal center.[15,41,44] The polymer molar mass values remain unchanged while, similarly to our results, the molar mass distribution becomes relatively narrower, going from 1.22 with pure toluene to 1.09 or 1.14 with THF or DME in 10%, respectively. Nevertheless, with our initiators, using an even more coordinating solvent such as CH_3CN seems unfavorable as observed on the molar mass distributions that may then broaden to 1.9. Therefore, THF as solvent appears to offer a good compromise between a strongly coordinating and a weakly coordinating solvent to achieve a quite controlled polymerization process.

Formation of a Gel. During the polymerization of ϵ-CL initiated by the borohydride complexes **Ln-1** and **Cp*$_2$Sm-1**,[1] under the experimental conditions used (Tables 1−3 and 5), the viscosity of the solution rapidly increases and finally, the solution ends up as a gel. This change in viscosity does not impede the complete conversion of the monomer nor does it alter the molar mass distribution. This gel which is thermally stable and which disappears upon hydrolysis is thus qualified as a "physical" gel. Dissolution of a P(ϵ-CL) sample in CH_2Cl_2, in the same concentration as that for which a gel is observed in the active system, shows the complete solubility of the polymer. Furthermore, performing the polymerization in the same solvent in more dilute conditions such that the potential interactions are considerably weakened does impede the formation of a

Table 4. Number of Growing Polymer Chains per Rare Earth Center in the Polymerization of ϵ-CL Initiated by $Ln(BH_4)_3(THF)_3$, Ln-1, in THF (Data Derived from Tables 1−3)

$Ln(BH_4)_3(THF)_3$	$[\epsilon\text{-CL}]_0/[BH_4]_0$	N^a	av value of N
$La(BH_4)_3(THF)_3$	>150	3.51	3.48
	<150	3.45	
$Nd(BH_4)_3(THF)_3$	>150	4.26	3.95
	<150	3.63	
$Sm(BH_4)_3(THF)_3$	>150	3.72	3.93
	<150	4.00	

[a] Number of polymer chains per Ln calculated by $\bar{M}_{n(theo)}/\bar{M}_{n(exp)}$ × number of active sites (3).

Table 5. Polymerization of ϵ-CL in CH_2Cl_2/Toluene (30/70) Initiated by $Sm(BH_4)_3(THF)_3$, Sm-1 (Polymerization Time = 10 min; $[\epsilon\text{-CL}]_0$ = 1128 mmol L^{-1}; Monomer Conversion = 100%)

$[\epsilon\text{-CL}]_0/[BH_4]_0$[a]	[**Sm-1**]$_0$ (mmol L^{-1})	$\bar{M}_{n(theo)}$[b] (g mol^{-1})	$\bar{M}_{n(exp)}$ (g mol^{-1})	$\bar{M}_w/\bar{M}_n$
377	1.0	42978	29600	1.4
269	1.4	30666	26700	1.4
157	2.4	17920	15600	1.5
108	3.5	12312	12450	1.4
59	6.4	6734	6350	1.3

[a] $[BH_4]_0 = 3[\textbf{Sm-1}]_0 = 3[Sm(BH_4)_3(THF)_3]_0$. [b] Calculated for three growing polymer chains per samarium atom with $\bar{M}_{n(theo)} = [\epsilon\text{-CL}]_0/[BH_4]_0$ × monomer conversion × 114.

Table 6. Solvent Effect on the Polymerization of ϵ-CL Initiated by $Sm(BH_4)_3(THF)_3$, Sm-1

solvent	$[\epsilon\text{-CL}]_0/[BH_4]_0$[a]	$[\mathbf{Sm\text{-}1}]_0$ (mmol L^{-1})	$[\epsilon\text{-CL}]_0$ (mmol L^{-1})	reacn time (min)	monomer convn[b] (%)	$\bar{M}_w/\bar{M}_n$
CH_2Cl_2/ toluene (30/70)	59	6.4	1128	2	100	1.3
THF	53	7.1	1128	5	100	1.2
CH_3CN	52	4.5	694	180	88	1.9

[a] $[BH_4]_0 = 3[\mathbf{Sm\text{-}1}]_0 = 3[Sm(BH_4)_3(THF)_3]_0$. [b] Determined by ^1H NMR.

Table 7. Polymerization of ϵ-CL in CH_2Cl_2 Initiated by $Sm(BH_4)_3(THF)_3$, Sm-1 (Polymerization Time = 10 min; Monomer Conversion[b] = 100%)

$[\epsilon\text{-CL}]_0/[BH_4]_0$[a]	$[BH_4]_0$ (mmol L^{-1})	$[\epsilon\text{-CL}]_0$ (mmol L^{-1})	$\bar{M}_{n(theo)}$[c] (g mol^{-1})	$\bar{M}_{n(exp)}$ (g mol^{-1})	$\bar{M}_w/\bar{M}_n$	N[d]
127	2.36	300	14478	14100	1.5	3.08
364	1.65	600	41500	39600	1.3	3.14

[a] $[BH_4]_0 = 3[\mathbf{Sm\text{-}1}]_0 = 3[Sm(BH_4)_3(THF)_3]_0$. [b] Determined by ^1H NMR. [c] Calculated for three growing polymer chains per samarium atom with $\bar{M}_{n(theo)} = [\epsilon\text{-CL}]_0/[BH_4]_0 \times 114$. [d] Number of polymer chains per Sm calculated by $\bar{M}_{n(theo)}/\bar{M}_{n(exp)} \times$ number of active sites (3).

gel (Table 7). It is noteworthy that, under such conditions, the agreement between the experimental and theoretical molar mass values is good.[60] In addition, we verified that the polymerization of ϵ-CL initiated by "Ln(OiPr)$_3$" (Ln = La, Sm), using the same monomer and initiator concentrations as with **Ln-1**, does not lead to the formation of a gel.

These results indicate first, that the gel is not due to a too high concentration of polymer in the reaction medium. Second, it implies that the cohesion of the gel is ensured by interactions only occurring with functions available in the active polymer system derived from borohydride precursors $Ln[O(CH_2)_5C(O)\{O(CH_2)_5C(O)\}_nO(CH_2)_5(OBH_2)]_3$, Ln = La, Nd, Sm).[1,2] These functions are neither present after the termination step nor in the active polymer systems issued from isopropoxide precursors $Ln[O(CH_2)_5C(O)\{O(CH_2)_5C(O)\}_nO(CH_2)_5(O^iPr)]_3$).[4] Considering the nature of these two types of active polymer chains, the $-(OBH_2)$ end group might thus well be implicated in the gel cohesion. Understanding the formation of such a gel in the active polymer is then essential for a deeper mechanistic approach required in order to access to macromolecular architectures such as copolymers.

B. Comparative IR Studies of the Intermediates of the Polymerization. Van der Waals Bonding Interactions Involving the —(OBH$_2$) Chain End Unit. Within the active polymers $Ln[O(CH_2)_5C(O)\{O(CH_2)_5C(O)\}_nO(CH_2)_6(OBH_2)]_3$, **Ln-3**, Ln = La, Nd, Sm, prepared from the borohydride initiators $Ln(BH_4)_3(THF)_3$, **Ln-1**, in addition to the rare earth metal which may interact with the various oxygen atoms of the polymer chain (not illustrated in Figure 4), the $-(O^{\delta-}-B^{\delta+}-H_2\ ^{\delta-})$ group might be involved in various inter- and intramolecular van der Waals interactions, as illustrated in Figure 4. We attempted to highlight the presence of such bonding interactions upon analyzing, through infrared spectroscopy, the various reaction intermediates formed during the polymerization process. Indeed, upon formation of the active polymer gels **Ln-3** (from **Ln-1** via $Ln[O(CH_2)_6(OBH_2)]_3$, **Ln-2**), significant changes in the vibration bands (wavenumber and intensity) of the B−H, C=O, O−CH_2, B−O, and Ln−O bonds should be expected. For such bonds involved in van der Waals interactions, a shift of the stretching frequencies to lower energy and of the deformation frequencies to higher energy should be

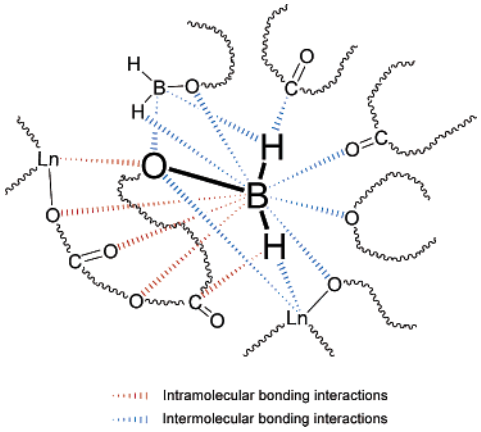

Figure 4. Potential van der Waals bonding interactions within the active polymer gel $Ln[\{O(CH_2)_5C(O)\}_nO(CH_2)_6(OBH_2)]_3$, **Ln-3**.

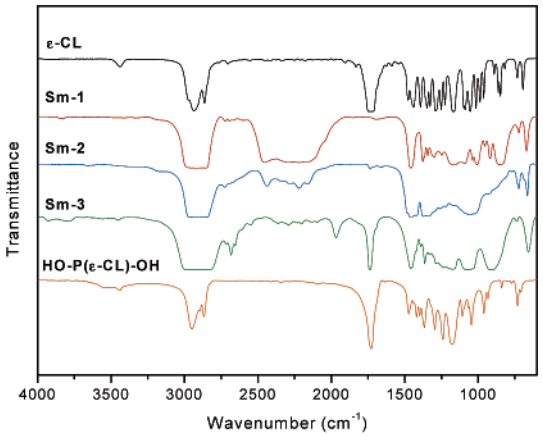

Figure 5. IR spectra of ϵ-CL, $Sm(BH_4)_3(THF)_3$, **Sm-1**, $Sm[O(CH_2)_6(OBH_2)]$, **Sm-2**, $Sm\{O(CH_2)_5C(O)\}_nO(CH_2)_6(OBH_2)$, **Sm-3**, and HO−P(ϵ-CL)−OH.

anticipated.[45−47] In the following discussion, all the data have been taken into account; yet, for clarity, only the most relevant results obtained from samarium are illustrated (Figure 5; all other data including those of the **Cp$_2$*Sm-1,2,3** system are given in the Supporting Information). These IR analyses of the newly isolated **Ln-2** and **Ln-3** samples along with the elemental analysis of **Ln-2** species further confirm the formulation of these intermediates.[1,2]

The B−H Bond. The trisborohydride complexes **Ln-1** have been characterized by their X-ray structure which displayed two tridentate and one bidentate ligands.[30,31,48−50] The IR spectra of **Ln-1,** recorded in the present work for reference, display three sets of bands corresponding to the $\nu(B-H_{terminal})$ (2454−2427 cm^{-1}), $\nu(B-H_{bridging})$ (2230−2110 cm^{-1}), and $\delta(B-H)$ (1167−1091 cm^{-1}), as found in the literature for La and Nd[30,48,49] and which is typical of rare earth metal borohydride complexes.[48,50−52]

Assignments of $\nu(B-H)$ and $\delta(B-H)$ initially made on complexes **Ln-1** and **Ln-2** have then allowed the

attributions of the bands in **Ln-3** to be derived. The ν(B−H) and δ(B−H) are getting weaker from **Ln-1** to **Ln-2**, to **Ln-3**, respectively. The very intense B−H stretching bands recorded in **Ln-1** (2454−2427 cm^{-1} and 2230−2110 cm^{-1}) clearly decrease in intensity to medium bands in **Ln-2** (2439−2317, 2294−2027 cm^{-1}) in agreement with the change from BH_4 to BH_2, and to weak bands in **Ln-3** (2369−2096 cm^{-1}) as anticipated on going to a longer polymer chain. The δ(B−H) deformation band (1167−1091 cm^{-1}) in **Ln-1** is hardly shifted to lower energy (1168−1031 cm^{-1}) in **Ln-2** spectra but clearly moves to higher energy (1335−1164 cm^{-1}) in **Ln-3**.

The C═O Bond. As expected for polyesters, the C═O group gives a strong stretching absorption typical of an ester linkage at 1737−1735 cm^{-1} for **Ln-3** and 1728 cm^{-1} for the HO−P(ϵ-CL)−OH (compared to 1724 cm^{-1} for ϵ-CL). Surprisingly, this ν(C═O) band is shifted to higher frequency and not to lower frequency, as expected if it were involved in van der Waals interactions. A weak ν(C═O) band is also observed in the IR spectra of the alkoxyborane intermediates **Ln-2** (1736−1734 cm^{-1}); this was unpredicted since these products are not supposed to contain any carbonyl group. Given the preparation of these **Ln-2** samples from **Ln-1** and ϵ-CL, this absorption can only arise from either intermediates $Ln(BH_4)_3(\epsilon\text{-CL})_3$ or $Ln[O(CH_2)_5C(O)(HBH_3)]_3$.[1,2] The occurrence of this absorption gives further evidence for the presence of the equilibrium between $Ln(BH_4)_3(\epsilon\text{-CL})$, $Ln[O(CH_2)_5C(O)(HBH_3)]_3$, and **Ln-2** as previously described.[1,2]

Thus, upon preparing **Ln-3** from **Ln-1** via **Ln-2**, concomitantly with the formation of a gel in the reaction medium, the most significant and relevant variations in the IR absorption frequencies of the various bonds are observed for the B−H and C═O bonds. Other bonds involved in these types of interactions (B−O, Ln−O, O−CH_2, or O−C(O)) could not give conclusive results for they were either not resolved or not observed (refer to the Supporting Information). While the ν(B−H) and δ(B−H) exhibit a bathochromic and hypsochromic shift respectively, as expected for "B−H" bonds involved in van der Waals interactions,[45−47] the ν(C═O) displays an hypsochromic shift. All these noteworthy differences among the IR spectra of the actives species **Ln-1,2,3**, the monomer ϵ-CL, and the polymer HO−P(ϵ-CL)−OH strongly suggested the presence of −(OBH_2) end group(s) involved in many van der Waals inter- and intramolecular bonding interactions in the active polymer chains **Ln-2** and **Ln-3**, according to Figure 4. These interactions are thus presumed to contribute to the gel formation observed during the polymerization of (ϵ-CL) initiated by the borohydride complexes **Ln-1**.

C. Transfer Reactions: a Consequence of van der Waals Interactions. As illustrated in Figure 4, each active polymer chain and especially the [Ln]−O polymerization site might be involved in many inter- and intramolecular interactions. One could thus easily envisage some transfer reaction(s) that would give a putative rare earth metal hydride or alkoxide species with termination of a polymer chain. This would then rationalize the discrepancy obtained at high $[\epsilon\text{-CL}]_0/[BH_4]_0$ ratios between the theoretical and experimental molar mass values illustrated in Figures 1−3. This would also agree with the observation that, as mentioned above, no gel is formed when the polymerization is done in a dilute reaction medium. The greater the dilution, the less likely the interactions and the transfer reaction(s) and consequently, the better the agreement between $\bar{M}_{n(exp)}$ and $\bar{M}_{n(theo)}$ values (Table 7).

Table 8. Rare Earth Metal Present in the Final P(ϵ-CL) Synthesized upon Polymerization of ϵ-CL Initiated by Rare Earth Borohydride Complexes

initiator	initial amount of Ln (ppm)[a]	residual amount of Ln (ppm)[b]	residual amount of Ln (%)[c]
$La(BH_4)_3(THF)_3$	5200	33	0.63
$Sm(BH_4)_3(THF)_3$	1600	4.1	0.26

[a] Calculated based on both the amount of initiator and monomer initially used. [b] Determined by elemental analysis. [c] Calculated from the residual amount of Ln/initial amount of Ln.

D. Biocompatible P(ϵ-caprolactone) Synthesized from Nontoxic Rare Earth Initiators. Aliphatic polyesters prepared by ROP of lactones are biocompatible and bioresorbable; they are used in biomedical as well as pharmaceutical domains, especially as sutures, implants, and controlled drug delivery systems.[17,53,54] To highlight that poly(ϵ-caprolactone) synthesized through ROP using rare earth metal borohydride initiators has some great potential, we have evaluated the residual amount of rare earth metal present in our final polymers prepared from $Ln(BH_4)_3(THF)_3$ initiators (Table 8). These preliminary values found below 0.6% are much lower than the amount of zinc (10%) found in the poly(lactide) prepared from $Zn[O(CH_2)_3NHC(O)(O^tBu)]$ and later on used for drug encapsulation.[8]

Very few toxicological data concerning the rare earth metal elements are available in the literature.[55,56,57,61] Data available on metal chlorides allow the comparison of rare earth metals and other metals commonly used in ROP of cyclic esters, namely aluminum, zinc and tin.[18] The median lethal doses show that $LaCl_3$ (4200 mg/kg) is less toxic compared to $AlCl_3$ (3700 mg/kg), $SnCl_2$ (700 mg/kg), or $ZnCl_2$ (350 mg/kg).[56] This agrees with our previous findings about the low cytotoxicity evaluated both in vitro and in vivo of (trimethylenecarbonate-*co*-ϵ-caprolactone) polymers prepared from rare earth metal alkoxides and used as nerve guides.[5,6] Therefore, the low content of residual nontoxic rare earth metals in our P(ϵ-CL) polymers does make them suitable for biomedical or biopharmaceutical applications.

Conclusion

The trivalent homoleptic rare earth metal borohydride complexes $Ln(BH_4)_3(THF)_3$, **Ln-1** (Ln = La, Nd, Sm), do efficiently polymerize ϵ-CL. These polymerizations can be qualified as pseudo-living since molar mass distributions are moderate ($\leq$1.3) and the initiators efficiency reaches 100% for various monomer-to-initiator ratios. The thorough IR investigations of the polymerization intermediates have revealed the occurrence of inter- and intramolecular van der Waals interactions involving the −(OBH_2) living polymer chain end. These interactions, in turn, induce some transfer reactions which are rather limited with lanthanum-based initiators (compared to neodymium or samarium ones) or in diluted medium. Finally, further support of the "livingness" of the P(ϵ-CL) chain end derived from borohydride complexes initiation is provided by the successful block copolymerization of cyclic esters, such as ϵ-CL−ϵ-CL− or ϵ-CL−TMC; these results will be presented in a forthcoming paper.

Supporting Information Available: Text giving experimental details for **Cp*$_2$Sm-1**, **Cp*$_2$Sm-2**, and **Cp*$_2$Sm-3** and comparative IR studies of $(Cp^*)_2Sm(BH_4)(THF)$, **Cp*$_2$Sm-1**, $(Cp^*)_2Sm(BH_4)(\epsilon\text{-CL})$, $(Cp^*)_2Sm[O(CH_2)_6(OBH_2)]$, **Cp*$_2$Sm-2**, and $(Cp^*)_2Sm[\{O(CH_2)_5C(O)\}_{95}O(CH_2)_6(OBH_2)]$, **Cp*$_2$Sm-3**, and of the B−O, Ln−O or O−CH_2, O−C(O), C−H, and C−C bonds in **Ln-1,2,3/Cp*$_2$Sm-1,2,3**, a figure showing compound formulas and numbering, and a figure showing the IR spectra of **Sm-2** and **Cp*$_2$Sm-2**. This material is available free of charge via the Internet at http://pubs.acs.org.

References and Notes

(1) Palard, I.; Soum, A.; Guillaume, S. M. *Chem.—Eur. J.* **2004**, *10*, 4054−4062.
(2) Guillaume, S. M.; Schappacher, M.; Soum, A. *Macromolecules* **2003**, *36*, 54−60.
(3) Save, M.; Soum, A. *Macromol. Chem. Phys.* **2002**, *203*, 2591−2603.
(4) Save, M.; Schappacher, M.; Soum, A. *Macromol. Chem. Phys.* **2002**, *203*, 889−899.
(5) Fabre, T.; Schappacher, M.; Bareille, R.; Dupuy, B.; Soum, A.; Bertrand-Barat, J.; Baquey, C. *Biomaterials* **2001**, *22*, 2951−2958.
(6) Schappacher, M.; Fabre, T.; Mingotaud, A.-F.; Soum, A. *Biomaterials* **2001**, *22*, 2849−2855.
(7) Caillol, S.; Lecommandoux, S.; Mingotaud, A.-F.; Schappacher, M.; Soum, A.; Bryson, N.; Meyrueix, R. *Macromolecules* **2003**, *36*, 1118−1124.
(8) Caillol, S.; Meyrueix, R.; Bryson, N.; Soum, A.; Soula, G.; Mingotaud, A.-F. FR 2 838 964; WO 03/090727, 2003.
(9) Yasuda, H. *Prog. Polym. Sci.* **2000**, *25*, 573−626.
(10) Hou, Z.; Wakatsuki, Y. *Coord. Chem. Rev.* **2002**, *231*, 1−22.
(11) Agarwal, S.; Mast, C.; Dehnicke, K.; Greiner, A. *Macromol. Rapid Commun.* **2000**, *21*, 195−212.
(12) Yasuda, H. *Topics Organomet. Chem.* **1999**, *2*, 255−283.
(13) Ravi, P.; Gröb, T.; Denicke, K.; Greiner, A. *Macromol. Chem. Phys.* **2001**, *202*, 2641−2647.
(14) Yamashita, M.; Takemoto, Y.; Ihara, E.; Yasuda, H. *Macromolecules* **1996**, *29*, 1798−1806.
(15) Ravi, P.; Gröb, T.; Dehnicke, K.; Greiner, A. *Macromolecules* **2001**, *34*, 8649−8653.
(16) Agarwal, S.; Puchner, M. *Eur. Polym. J.* **2002**, *38*, 2365−2371.
(17) Albertsson, A.-C.; Varma, I. K. *Biomacromolecules* **2003**, *4*, 1466−1486.
(18) Stridsberg, K. M.; Ryner, M.; Albertsson, A.-C. *Adv. Polym. Sci.* **2002**, *157*, 42−65.
(19) Shen, Y.; Shen, Z.; Zhang, Y.; Yao, K. *Macromolecules* **1996**, *29*, 8289−8295.
(20) Penczek, S.; Szymanski, R.; Duda, A.; Baran, J. *Macromol. Symp.* **2003**, *201*, 261−269.
(21) Hultzch, K. C.; Okuda, J. *Macromol. Rapid Commun.* **1997**, *18*, 809−815.
(22) Gröb, T.; Seybert, G.; Massa, W.; Weller, F.; Ravi, P.; Greiner, A.; Dehnicke, K. *Angew. Chem.* **2000**, *39*, 4373−4375.
(23) Shen, Y. Q.; Shen, Z. Q.; Zhang, F. Y.; Zhang, Y. F. *Polym. J.* **1995**, *27*, 59−64.
(24) Kricheldorf, H. R.; Sumbel, M. V. *Makromol. Chem.* **1998**, *189* (2), 317−331.
(25) Dunsing, R.; Kricheldorf, H. R. *Eur. Polym. J.* **1988**, *24*, 145−150.
(26) Kricheldorf, H. R.; Joerg, J. *Macromol. Sci., Chem.* **1989**, *A26* (4), 631−644.
(27) *The Chemist's Companion*, 1st ed.; Gordon, A. J., Ford, A., Eds.; Wiley-Interscience: New York, 1972.
(28) Cendrowski-Guillaume, S. M.; Le Gland, G.; Nierlich, M.; Ephritikhine, M. *Organometallics* **2000**, *19*, 5654−5660.
(29) Cendrowski-Guillaume, S. M.; Nierlich, M.; Lance, M.; Ephritikhine, M. *Organometallics* **1998**, *17*, 786−788.
(30) *Gmelin Handbook of Inorganic and Organometallic Chemistry*, Springer-Verlag: Berlin, 1991; RE Main Vol. C 11 b, pp 480−487.
(31) Mirsaidov, U.; Shaimuradov, I. B.; Khikmatov, M. *Russ. J. Inorg. Chem.* **1986**, *31*, 753−754.
(32) Chen, J.-L.; Yao, Y.-M.; Luo, Y.-J.; Zhou, L.-Y.; Zhang, Y.; Shen, Q. *J. Organomet. Chem.* **2004**, *689*, 1019−1024.
(33) Yu, C.; Zhang, L.; Shen, Z. *Eur. Polym. J.* **2003**, *39*, 2035−2039.
(34) Fan, L.; Zhang, L.; Shen, Z. *Polym. J.* **2004**, *36*, 91−95.
(35) Ling, J.; Shen, Z.; Huang, Q. *Macromolecules* **2001**, *34*, 7613−7616.
(36) Zhang, L.; Shen, Z.; Yu, C.; Fan, L. *J. Mol. Catal.* **2004**, *214*, 199−202.
(37) Yu, C.; Zhang, L.; Shen, Z. *J. Mol. Catal.* **2004**, *212*, 365−369.
(38) Agarwal, S.; Mast, C.; Anfang, S.; Karl, M.; Denicke, K.; Greiner, A. *Polym. Prepr.* **1998**, *39*, 414−415.
(39) Kerton, F. M.; Whitwood, A. C.; Willians, C. E. *J. Chem. Soc., Dalton Trans.* **2004**, 2237−2244.
(40) Ma, H.; Spaniol, T. P.; Okuda, J. *Dalton Trans.* **2003**, 4770−4780.
(41) Dehnicke, K.; Greiner, A. *Angew. Chem., Int. Ed.* **2003**, *42*, 1340−1354.
(42) Evans, W. J.; Fujimoto, C. H.; Johnston, M. A.; Ziller, J. W. *Organometallics* **2002**, *21*, 1825−1831.
(43) Agarwal, S.; Karl, M.; Dehnicke, K.; Seybert, G.; Massa, W.; Greiner, A. *J. Appl. Polym. Sci.* **1999**, *73*, 1669−1674.
(44) Agarwal, S.; Karl, M.; Anfang, S.; Dehnicke, K.; Greiner, A. *Polym. Prepr.* **1998**, *38*, 361−362.
(45) Pavia, D. L.; Lampman, G. M.; Kriz, G. S. Jr., In *Introduction to Spectroscopy*; Saunders College: Philadelphia, PA, 1979; Chapter 2, pp 13−73.
(46) Siesler, H. W.; Holland-Moritz, K. In *Infrared and Raman Spectroscopy of Polymers, Practical Spectroscopy*; Brame, E. G., Jr., Ed.; Marcel Dekker Inc.: New York, 1980. Chapter 4, pp 219−227.
(47) March, J. *Advanced Organic Chemistry*, 4th ed.; Wiley-Interscience: New York, 1992; Chapter 3, pp 75−79.
(48) Makhev, V. D. *Russ. Chem. Rev.* **2000**, *69*, 727−746.
(49) Mirsaidov, U.; Shaimuradov, I. B.; Khikmatov, M. *Russ. J. Inorg. Chem.* **1986**, *31*, 753−754.
(50) Greenwood, N. N. *Coord. Chem. Rev.* **2002**, *226*, 61−69.
(51) Marks, T. J.; Kolb, J. R. *Chem. Rev.* **1977**, *77*, 263−292.
(52) Ephritikhine, M. *Chem. Rev.* **1997**, *97*, 2193−2242.
(53) Albertsson, A.-C. *Adv. Polym. Sci.* **2002**, *157*, 1−40.
(54) Okada, M. *Polym. Sci.* **2002**, *27*, 87−133.
(55) Hirano, S.; Suzuki, K. T. *Envir. Health Persp.* **1996**, *104*, 85−95.
(56) Saxs, N. I. *Dangerous properties of industrial materials*, 6th ed.; Van Nostrand Reinhold Company: New York, 1984.
(57) Haley, P. J. *Health Phys.* **1991**, *61*, 809−820.
(58) Indeed, the $Ln(BH_4)_3(THF)_3$, **Ln-1**, complexes have been characterized by their X-ray crystallographic structures, which showed that the compounds, in the solid state, are monomeric and display one bidentate and two tridentate borohydride ligands as $Ln[(\mu_2\text{-}H)_3BH]_2[(\mu_2\text{-}H)_2BH_2](THF)_3$ (as illustrated in Scheme 1).[30,31] In addition, the ^1H NMR spectra of these complexes confirm the presence of three (BH_4) groups as well as three THF molecules per rare earth metal.
(59) For instance, within the $Ln(OR)_3$ initiator series published by Shen, the activity of $Ln(O^iPr)_3$ follows the decreasing order La > Pr > Nd > Gd > Dy > Y[23] while the more sterically crowded initiator Ln(4-*tert*-butylphenolate)$_3$ also displays the same tendency (La > Gd > Nd > Sm >Y > Er).[33,37] However, in the former study using $Ln(O^iPr)_3$, the molar mass distribution with lanthanum reaches 2.04 while that with yttrium is only 1.20.[23] Greiner has observed that the yields and molar mass values of the P(ϵ-CL) polymers formed from $LnCl_3$ are lower with $SmCl_3$ or $LuCl_3$ as compared to $CeCl_3$ (Ce > Sm ∼ Lu; cerium being the largest metal) while the molar mass distribution remain alike.[38]
(60) Note that since it requires extreme purification of the reagents to perform the polymerization experiments under such diluted conditions using a rare earth metal borohydride initiator, these were not done on a regular basis.
(61) In the biological system, the metabolic fate of the rare earth metal appears to be governed by the solubility of the rare earth metal complex. Generally, the toxicity of rare earth elements decreases across the series (with the atomic number), most likely as the result of a greater solubility and ionic stability of heavier metals.[57] Yet, because rare earth metals exhibit analogous chemical properties throughout the series, it is feasible that their binding affinities to biomolecule, their metabolisms, and toxicities in the living system are also very similar.[55] Mortality studies have revealed that these metals are not highly toxic; the median lethal dose values for intravenously injected rare earth metals are 10−100 mg/kg of body weight and those of intraperitoneally injected rare earth metals are 150−700 mg/kg of body weight.[57]

MA0506280